Anisotropic Fluorescence Emission of Ionic Complex Induced by the Orientation of Azobenzene Unit

ARTICLE *in* MACROMOLECULES · MAY 2013

Impact Factor: 5.8 · DOI: 10.1021/ma400247h

5 AUTHORS, INCLUDING:

Xuemin Lu
Shanghai Jiao Tong University
56 PUBLICATIONS **447** CITATIONS
SEE PROFILE

Feng Shan
Shanghai Jiao Tong University
8 PUBLICATIONS **57** CITATIONS
SEE PROFILE

Qinghua Lu
Shanghai Jiao Tong University
128 PUBLICATIONS **2,667** CITATIONS
SEE PROFILE

Macromolecules

Article

pubs.acs.org/Macromolecules

Anisotropic Fluorescence Emission of Ionic Complex Induced by the Orientation of Azobenzene Unit

Jun Wu, Xuemin Lu,* Zeyuan Yi, Feng Shan, and Qinghua Lu*

School of Chemistry and Chemical Engineering, the State Key Laboratory of Metal Matrix Composites, Shanghai Jiao Tong University, Shanghai 200240, P. R. China

Supporting Information

ABSTRACT: A series of azobenzene-containing fluorescent complexes with stilbene fluorescent unit were prepared based on the ionic self-assembly approach. The incorporation of the stilbene unit did not change the lamellar structure of the azobenzene-containing complex. Under pulsed laser irradiation, the azobenzene group oriented in the direction perpendicular to the laser polarization, and as a result, the fluorescent stilbene unit was cooperatively oriented following the direction of azobenzene group orientation. This oriented complex films presented anisotropic emission of fluorescence, and the anisotropic ratio of fluorescence increases with the increase of the content of azobenzene unit in the complex.

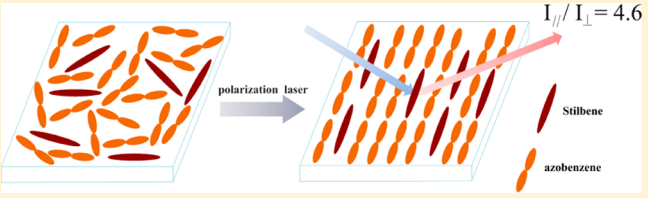

INTRODUCTION

Materials with anisotropic fluorescence emission played a key role in constructing LED as light source in the fast developing field of flat display technologies.[1,2] A direct approach to prepare materials with anisotropic fluorescence emission is to align the fluorescent units in a desired direction. In the case of polymer materials, orientation of fluorescent unit to obtain high polarization ratio can be carried out by a variety of methods such as stretching,[3] rubbing,[4,5] Langmuir−Blodgett (LB) film,[6−8] electrospinning,[9−11] etc. However, mechanical damaging and time-consuming often occurred among these methods.

Recently, orientation of the fluorescent unit driven by a photosensitive unit has received intensive attention due to its noncontact alignment nature.[12−14] In such an approach, the fluorescent unit was cooperatively oriented following the photoactive movement of the photosensitive molecules. For example, Stumpe et al. investigated the cooperative orientation of photosensitive cinnamate group and different dye units under light irradiation and the photosensitive polymer emitted polarized light with a high dichroic ratio.[15] Lee et al. also reported a series of supramolecules comprised of fluorenevinylene and cinnamate side group in which the fluorenevinylene was cooperatively oriented by the cinnamate group.[16,17]

As a well-known kind of photosensitive molecule, azobenzene and its derivatives have been intensively investigated for their reversible *cis*−*trans* isomerization under light irradiation.[18−22] A much higher order parameter of azobenzene group can be easily obtained compared with other photosensitive group. However, few reports were presented using its photoinduced alignment to drive the orientation of fluorescent unit. This was a point of view most of people thought that the emission of organic fluorescent molecule was quenched while adding the azobenzene molecules into the fluorescent polymer film due to the energy transfer process or oxidative/reductive electron transfer process.[23−25] In fact, the quenching effects only can occur under certain condition, such as the overlap integral between the fluorescence and the azobenzene unit,[26,27] certain chemical structures of the chromophores,[28,29] and special microstructure of the matrix.[30−32] Therefore, whether the fluorescence quenching can be avoided through appropriate molecular design and the polarized fluorescence film with high orientation of fluorescence can be obtained with the aid of photoinduced azobenzene orientation are still worthy of further exploration.

In this work, we reported the photoinduced cooperative orientation of fluorescent unit, stilbene molecule, in an azobenzene-containing polymer matrix prepared by the ionic self-assembly (ISA) approach. This fluorescent ionic complex shows lamellar structure and meagerly quenching effect on the fluorescence emission. Under laser irradiation, the fluorescent unit and the azobenzene group present cooperative orientation in the same direction, perpendicular to the laser polarization. Consequently, a dichroic ratio of fluorescent emission up to 4.6 was obtained from this kind of fluorescent complex.

EXPERIMENTAL SECTION

Materials. Poly(acrylic acid) (PAA) aqueous solution (25 wt %, M_w 240 000) was purchased from Alfa Aesar. Sodium polyacrylate was obtained from the neutralization of PAA with sodium hydroxide. Sodium nitrite, phenol, potassium carbonate, 4-methoxyaniline, 33 wt % trimethylamine alcoholic solution, piperidine, and organic solvents involved in this work were purchased from the Sinopharm Chemical Reagent Co. *N*-Methyl-*N*-(2-hydroxyethyl)-4-aminobenzaldehyde, 4-nitrophenylacetic acid, 1,6-dibromohexane, and 6-bromohexanoyl chloride were obtained from J&K Reagent Co. All the reagents were

Received: February 2, 2013
Revised: April 12, 2013
Published: April 25, 2013

Scheme 1. Synthetic Route to the Fluorescence Unit (Nstil) and Azobenzene Moiety (MAZO)

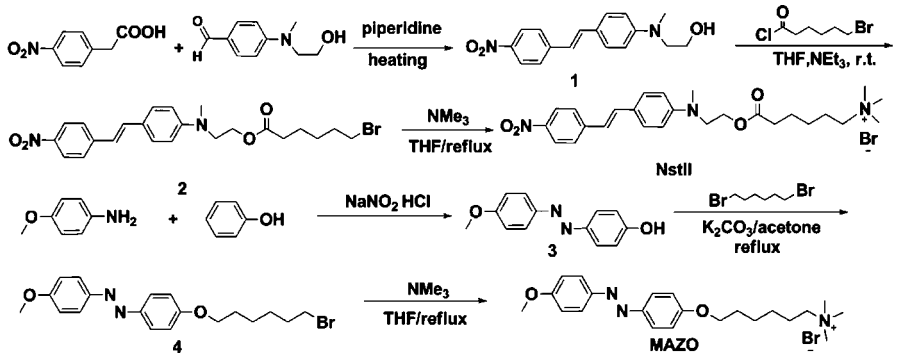

used without further purification unless stated otherwise. 4-(*N*-(2-Hydroxyethyl)-*N*-methylamino)-4′-nitrostilbene (**1**) and trimethyl-6-(4-methoxyazobenzene-4′-oxy)hexylammonium bromide (MAZO) were synthesized according to the reported methods.[33−35]

2-(N-Methyl-N-(4-nitrostilbene)-4′-amino)ethyl 6-Bromohexanoate (2). To a solution of **1** (1.00 g, 3.36 mmol) in 40 mL of dry THF, triethylamine (470 mg, 4.70 mmol, 1.4 equiv) was added at room temperature, and the solution was stirred for 15 min. The reaction mixture was cooled to 0 °C in an ice bath, and 6-bromohexanoyl chloride (1.00 g, 4.70 mmol, 1.4 equiv) was added slowly by syringe. The resulting mixture was heated to room temperature and stirred for 24 h. After filtration, the filtrate was evaporated by vacuum at room temperature. The residue was dissolved in ethyl acetate and washed with deionized water for three times. Then organic layer was dried using anhydrous $MgSO_4$. The dark brown solid product was obtained after evaporating the solvent and further purified by column chromatography on a SiO_2 column. Yield 1.15 g, 72%. ^{1}H NMR (400 MHz, $CDCl_3$, δ (ppm)): 8.17−8.19 (d, 2H), 7.55−7.58 (d, 2H), 7.43−7.45 (d, 2H), 7.18−7.20 (d, 1H), 6.91−6.95 (d, 1H), 6.73−6.76 (d, 2H), 4.27−4.30 (t, 2H), 3.64−3.57 (t, 2H), 3.35−3.38 (t, 2H), 3.04 (s, 3H), 2.25−2.29 (t, 2H), 1.55−1.61 (m, 2H), 1.42−1.44 (m, 2H), 1.22−1.25 (m, 2H).

Trimethyl-5-(2-(N-Methyl-N-(4-nitrostilbene)-4′-amino)-ethoxycarbonyl)amylammonium Bromide (Nstil). 1.1 g (2.32 mmol) of **2** was dissolved in 50 mL of tetrahydrofuran. To the solution, 4.15 g (23.2 mmol) of 33 wt % trimethylamine alcoholic solution was added, and the solution was refluxed for 48 h under dry nitrogen. The crude product was washed thoroughly with ethyl acetate to remove the unreacted material. Yield: 1.05 g, 85%. ^{1}H NMR (400 MHz, DMSO-d_6, δ (ppm)): 8.16−8.18 (d, 2H), 7.73−7.76 (d, 2H), 7.48−7.50 (d, 2H), 7.39−7.43 (d, 1H), 7.08−7.13 (d, 1H), 6.74−6.76 (d, 2H), 4.18−4.21 (t, 2H), 3.62−3.65 (t, 2H), 3.17−3.21 (m, 2H), 3.98 (s, 9H), 2.95 (s, 3H), 2.19−2.26 (t, 2H), 1.58−1.62 (m, 2H), 1.46−1.50 (m, 2H), 1.16−1.22 (m, 2H).

Synthesis of Ionic Complexes (PM*m*N*n*) and Films. The letters "*m*" and "*n*" in the abbreviation PM*m*N*n* denote that the molar ratio of the azobenzene moiety MAZO to the luminescence moiety Nstil in the complex is *m*:*n*. Take $PM_{0.8}N_{0.2}$ as an example; 0.107 g (0.2 mmol) of Nstil was dissolved in 40 mL of 70 °C water, and then the hot solution was added slowly to a 10 mL (10 mg mL^{-1}, 1 mmol of acrylate groups calculated by the polymer repeating unit) sodium polyacrylate (PANa) aqueous solution with vigorous stirring in a 300 mL beaker. The mixture was kept at 70 °C. In another beaker, 0.360 g (0.8 mmol) of MAZO was dissolved in 150 mL of hot water. Then the previous solution was added dropwise to the MAZO hot aqueous solution. The resulting precipitate was collected by filtration and washed thoroughly with deionized water to remove residual salts and noncomplexed precursors and then dried in vacuum at 60 °C for 24 h. The molar ratio of PANa, MAZO, and Nstil was 10:8:2. The PM*m*N*n* films were prepared by spin-coating a NMP solution (concentration: 40 mg mL^{-1}) onto a quartz plate, glass slide, and silica substrates and further dried in vacuum at 70 °C for 8 h to remove the residual solvent. The thickness of the resultant film was about 800−1000 nm measured by using UV−vis interferometry (model F20, Filmetrics, Inc.).

Instruments and Characterization. FTIR spectra were recorded on a PerkinElmer Spectrum 100 FTIR spectrometer on pressed thin transparent disks of the samples mixed with KBr. Nuclear magnetic resonance (^{1}H NMR) studies were carried out with a Varian Mercury Plus 400 MHz spectrometer using DMSO-d_6 or $CDCl_3$ as solvent at room temperature, and the chemical shifts were referenced relative to tetramethylsilane. Thermogravimetric analysis (TGA) was performed using a TA TGA Q5000IR instrument. Samples were heated at the speed of 20 °C min^{-1} from room temperature to 700 °C in nitrogen. Differential scanning calorimetry was performed on a TA DSC Q2000 instrument with a heating rate of 10 °C min^{-1} in nitrogen. Polarized optical microscopy (POM) was performed on a Leica DMLO microscope with a Leitz 350 hot stage. Small-angle X-ray scattering (SAXS) experiments were carried out on an Anton Paar SAXS instrument at room temperature. Wide-angle X-ray diffraction (WXRD) was performed on a Rigaku D/MAX-2200/PC diffractometer at 25 °C (Cu Kα radiation λ = 0.154 nm, U = 40 kV, I = 20 mA). The samples were obtained by the solution casting method. The solvent was volatilized slowly under 60 °C for 24 h and further dried in vacuum at 70 °C overnight. Absorption spectra of the PM*m*N*n* films and solution were performed on PerkinElmer LAMBDA 750 UV−vis and 20 UV−vis spectrophotometers, respectively. The degree of molecular orientation was evaluated by the polarized UV−vis spectra using a PerkinElmer LAMBDA 750 UV−vis spectrophotometer with polarization angle scanning from 10° to 330° equipped with a polarizer.

Photoinduced Orientation of the Complexes under Laser Irradiation. The photoinduced orientation experiment was done with an s-polarized Nd:YAG laser (355 nm), with a pulse duration of 5 ns and repetition rate of 10 Hz . The spin-coated films were fixed on an X−Y moving platform with the speeds being 0.1 and 5 mm s^{-1} in X and Y directions, respectively. The incident angle θ was fixed at 15° with respect to the normal of the PM*m*N*n* films.

The photoinduced orientation in the PM*m*N*n* films was evaluated by the in-plane order parameter (S) by

$$S = \frac{A_{\parallel} - A_{\perp}}{A_{\text{large}} + 2A_{\text{small}}}$$

where $A_{\parallel}$ and $A_{\perp}$ are the UV−vis absorbance of parallel and perpendicular to laser polarization direction (E), respectively. A_{large} and A_{small} are associated with the larger and smaller absorbance between $A_{\parallel}$ and $A_{\perp}$.

Fluorescence Properties of the Complexes. Fluorescence spectra of the films and solution were recorded with a PTI steady-state and time-resolved fluorescence spectrofluorometer (QM/TM/IM), and polarized excited photoluminescence measurements of the films were performed on the same instrument equipped with a polarizer. The complex films, spin-coated from the NMP solution with the same concentration of PM*m*N*n* (wt %), were used to test the fluorescent intensity (excitation slit: 12 nm; emission slit: 16 nm), the excitation wavelength was 470 nm. In order to comparison, the

dx.doi.org/10.1021/ma400247h | *Macromolecules* 2013, 46, 3376−3383

Scheme 2. Synthetic Route to the Ionic Complexes PM*m*N*n*

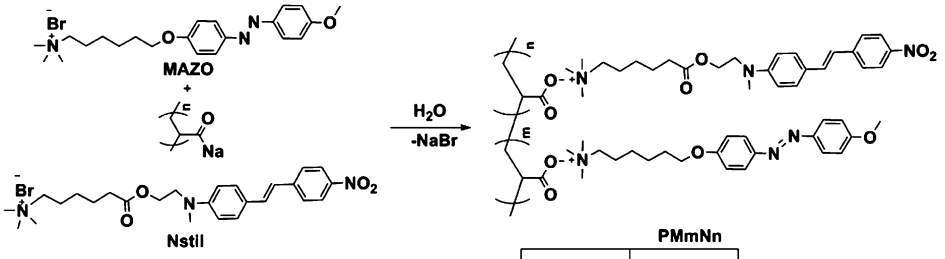

PMmNn	
m:n = 9:1	$PM_{0.9}N_{0.1}$
m:n = 8:2	$PM_{0.8}N_{0.2}$
m:n = 7:3	$PM_{0.7}N_{0.3}$
m:n = 6:4	$PM_{0.6}N_{0.4}$

fluorescence of PM*m*N*n* complex was also measured in the NMP solution with the same concentration of Nstil unit (0.5 mmol L^{-1}), which was calculated by the average molecule weight of repeating unit. Excitation and emission slits were set to 6 and 12 nm, respectively. The excitation wavelength was 550 nm. The fluorescence dichroic ratio R_{ex} was calculated by the equation

$$R_{ex} = I_{\parallel}/I_{\perp}$$

where $I_{\parallel}$ and $I_{\perp}$ are the fluorescence intensity measured in the direction parallel and perpendicular to the direction of laser polarization orientation, respectively. R_{ex} is calculated at maximum emission of the irradiated film by polarized fluorescence spectra.

Cyclic Voltammetry (CV). Cyclic voltammetry experiments were performed on CHI 630E electrochemical analyzer (Shanghai Chenhua Co.) for compounds **2** and **4** in THF solution at room temperature. 0.1 M tetrabutylammonium hexafluorophosphate was added to the THF solution as supporting electrolytes. The working electrode was a platinum electrode. A platinum spiral was used as the counter electrode and Hg/Hg_2Cl_2 electrode was used as the reference electrode. The scan rate was 50 mV s^{-1}.

RESULTS AND DISCUSSION

Synthesis and Characterization of Nstil, MAZO, and PM*m*N*n*. FTIR and ^{1}H NMR were used to confirm the successful formation of PM*m*N*n* complexes. As shown in Figure 1, the stretching vibration band of the carbonyl group in the

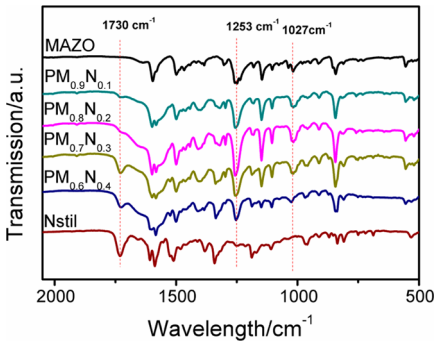

Figure 1. FT-IR spectra of $PM_{0.9}N_{0.1}$, $PM_{0.8}N_{0.2}$, $PM_{0.7}N_{0.3}$, $PM_{0.6}N_{0.4}$, MAZO, and Nstil.

stilbene unit was found in 1730 cm^{-1} whose intensity increased with the content of Nstil unit increasing. In addition, the stretching vibration bands of C=C double bonds in phenyl group were also found at ca. 1602 and 1500 cm^{-1}. The absorption band at 1340 cm^{-1} was associated with the stretching vibration of nitro group. Moreover, the absorption band of symmetric and asymmetric vibrations of Ar−O from MAZO unit was found at 1253 and 1027 cm^{-1}, respectively. These results confirmed the success attachment of Nstil and MAZO units to the PANa backbone.

Figure 2 presents the ^{1}H NMR spectra of the MAZO, Nstil, and PM*m*N*n* complexes. Take $PM_{0.6}N_{0.4}$ as an example; all the

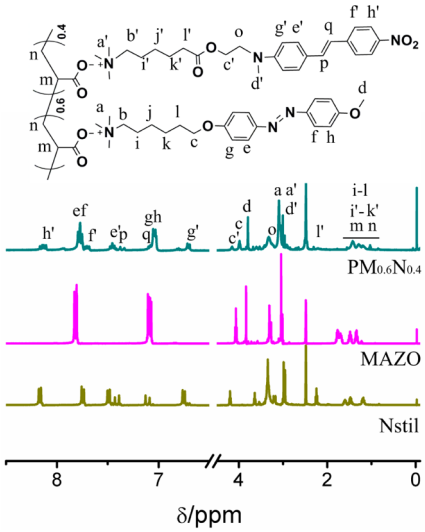

Figure 2. ^{1}H NMR spectra of $PM_{0.6}N_{0.4}$, MAZO, and Nstil.

proton signals were marked clearly. The proton signals of the phenyl groups in the MAZO and Nstil moieties corresponded to the chemical shifts of low-field region (>5 ppm) in the complex, while the chemical shifts of high-field region (<5 ppm) were from the proton signal of the polyelectrolyte main chain, the soft spacer, and methyl of the MAZO and Nstil moieties in the side chain. Compared to signal from the MAZO and Nstil, the proton signals form the $PM_{0.6}N_{0.4}$ complex had a slight shift, especially for the quaternary ammonium proton signals in the MAZO and Nstil moieties, indicating that the chemical environment of the protons changes slightly due to the formation of complex PM*m*N*n*. Moreover, the proton signals from the side-chain moieties became broader than the signal from the resource molecules MAZO and Nstil. These results above presented powerful evidence that the small molecules had attached to PANa main chain successfully. Furthermore, due to the partial overlap of the proton signals of MAZO and Nstil units in PM6N4, the overall peaks area of "*e*", "*f*", and "*f*'" had been integrated, which was as 4 times as the

dx.doi.org/10.1021/ma400247h | *Macromolecules* 2013, 46, 3376−3383

peak area of "h'". So the exact ratio of MAZO unit to Nstil unit in the complex $PM_{0.6}N_{0.4}$ was calculated to be 6:4.

To further confirm the ratio of the MAZO and Nstil units in the complexes, UV−vis absorption spectra of MAZO, Nstil, and PM*m*N*n* have been measured in NMP solutions (Figure 3).

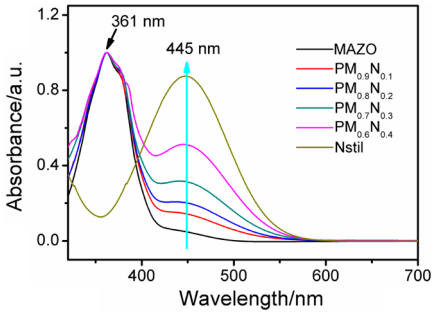

Figure 3. Normal UV−vis spectra of MAZO, $PM_{0.9}N_{0.1}$, $PM_{0.8}N_{0.2}$, $PM_{0.7}N_{0.3}$, and $PM_{0.6}N_{0.4}$ and Nstil in NMP solution.

MAZO and Nstil showed their absorption peaks at 361 and 445 nm, respectively. Therefore, the absorption band at 361 nm of PM*m*N*n* was attributed to the absorption of MAZO. Meanwhile, the absorption band at 445 nm was mainly associated with the absorption of Nstil unit and partly with the n−π^* transition of MAZO unit. The absorption at 445 nm (A_{445nm}) increased with the content of Nstil in PM*m*N*n* while normalizing the absorption at 361 nm (A_{361nm}). In addition, the UV−vis spectra of the mixture of MAZO and Nstil have also been measured in NMP solution (Figure S2 in Supporting Information). The mixture (abbreviated with M*m*N*n*, the "*m*" and "*n*" here indicate that the molar ratio of MAZO to Nstil in the mixture was *m*:*n*) showed two absorption peaks at 361 and 445 nm like PM*m*N*n*. According to Lambert−Beer's law, the concentration is proportional to the absorbance. Therefore, the ratio value A^*_{445nm}/A^*_{361nm} represents the concentration ratio of Nstil to MAZO unit in the complex. The detailed calculations for A^*_{445nm}/A^*_{361nm} of PM*m*N*n* and M*m*N*n* are shown in the Supporting Information, and their values are also collected in Table S1. A calibration curve was obtained from the mixture M*m*N*n* for the A^*_{445nm}/A^*_{361nm} value vs the content of Nstil in the complexes (Figure S2). The A^*_{445nm}/A^*_{361nm} value of $PM_{0.8}N_{0.2}$ and $M_{0.8}N_{0.2}$ was 0.135 and 0.131, respectively, which indicated the ratio of MAZO to Nstil moiety in $PM_{0.8}N_{0.2}$ was 8:2. Similar results were observed when other complexes were submitted to the same treatment. These results are consistent with that from ^{1}H NMR, indicating that the MAZO and Nstil attached to PANa backbone according to the initial calculated proportion.

Thermal Analysis and Phase Behavior. TGA and DSC were employed to investigate the stability and phase behavior of the complexes. TGA results showed that all the complexes were stable up to 165 °C (Figure S3). In order to avoid the interference of the thermal history, DSC thermograms of the second heating and cooling curves of PM*m*N*n* were employed. All of the complexes displayed two clear phase transition processes during the heating (Figure S4b) and cooling process (Figure 4), indicating their liquid crystalline behavior existing. The different textures could be observed reversibly by POM during the heating and cooling process, as shown in the Figure 4. The POM images were captured at the temperatures between the two peaks of the DSC second cooling curves, which further confirmed their liquid crystalline properties of the

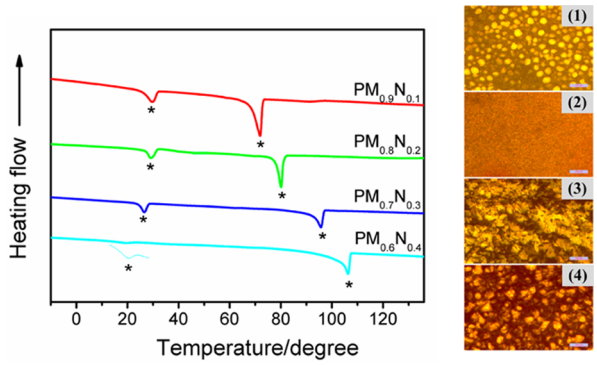

Figure 4. (left) DSC thermograms of the second cooling curves of PM*m*N*n* with the cooling rate being 10 °C min^{-1}. (right) POM images of PM*m*N*n* power obtained during cooling from their isotropic phase at the temperature 43, 70, 49, and 47 °C for $PM_{0.9}N_{0.1}$ (1), $PM_{0.8}N_{0.2}$ (2), $PM_{0.7}N_{0.3}$ (3), and $PM_{0.6}N_{0.4}$ (4), respectively. The bar is 100 μm.

complexes. The clearing points of the liquid crystalline complexes were in the range of 72 °C ($PM_{0.9}N_{0.1}$) to 105 °C ($PM_{0.6}N_{0.4}$) depending on the content of Nstil moieties (Table 1), and the liquid crystal temperature range became wide with

Table 1. Layer Spacing *d* Calculated from SAXS Profiles, Phase Transition Temperature, and Corresponding Enthalpy (ΔH) in the Cooling Process of the Ionic Complexes PM*m*N*n*

complexes	*d* (nm)	phase transition temp[a] (°C)	corresponding ΔH (J g^{-1})[b]
$PM_{0.9}N_{0.1}$	2.94	I 72 Sm 29 Cr	7.66, 1.98
$PM_{0.8}N_{0.2}$	3.01	I 80 Sm 29 Cr	4.40, 1.15
$PM_{0.7}N_{0.3}$	3.16	I 95 Sm 26 Cr	3.89, 1.10
$PM_{0.6}N_{0.4}$	3.27	I 105 Sm 22 Cr	7.59, 0.76

[a]Cr = crystalline phase; Sm = smectic phase; I = isotropic phase. Transition temperatures are the peak temperature of second cooling curves of DSC profiles. [b]Enthalpies are also calculated from DSC profiles.

the content of Nstil unit in PM*m*N*n* increasing. In addition, the low enthalpy change of $PM_{0.6}N_{0.4}$ from liquid crystalline phase to crystalline phase indicated the low degree of crystallization (Table 1).

The complexes PM*m*N*n* were further submitted to SAXS measurement to investigate their microstructure. Take $PM_{0.9}N_{0.1}$ as an example; two clear scattering peaks at q_1 = 2.13 nm^{-1} and q_2 = 4.26 nm^{-1} can be detected in the SAXS pattern (Figure 5a), indicating the presence of only one long-range lamellar microstructure with a spacing d = 2.94 nm ($d = 2\pi/q_1$). The d value was larger than the calculated molecular length for the fully extended side-chain unit of MAZO (2.39 nm) or Nstil (2.75 nm), revealing a partial interdigitated structure (Figure 5b). This result was similar to the previous report where a lamellar microstructure with partly overlap of side chain was postulated in the ionic complexes.[36,37] Furthermore, due to the incorporation of Nstil unit, the space d increased linearly in the following order: $PM_{0.9}N_{0.1}$ < $PM_{0.8}N_{0.2}$ < $PM_{0.7}N_{0.3}$ < $PM_{0.6}N_{0.4}$. WXRD analysis (Figure S6) showed a broad peak at wide angle 20° and several sharp peaks, indicating that the crystalline exists in the complexes and the degree of crystallization decreased with the content of Nstil unit increasing in PM*m*N*n*.

dx.doi.org/10.1021/ma400247h | *Macromolecules* 2013, 46, 3376−3383

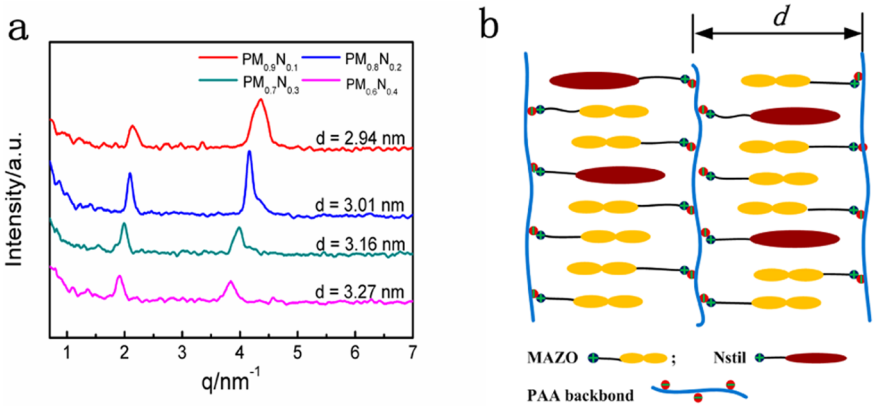

Figure 5. (a) SAXS patterns of PM*m*N*n* at room temperature after annealing at 70 °C for 10 h. (b) Possible molecular packing mode for the PM*m*N*n* complexes.

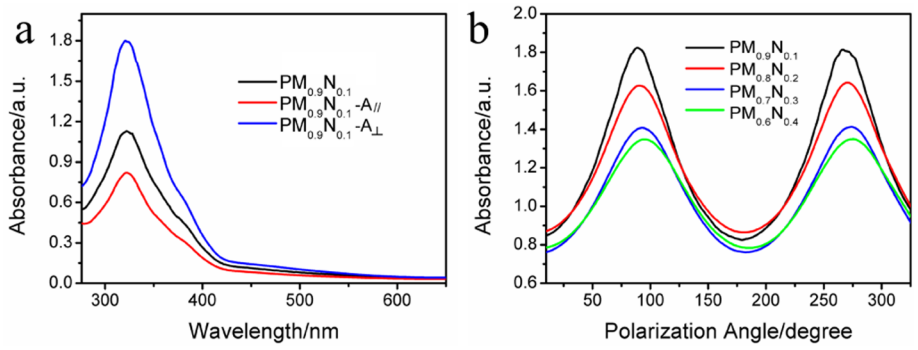

Figure 6. (a) Changes of polarized absorption spectra in the film of $PM_{0.9}N_{0.1}$ irradiated with 35 mW cm^{-2}. $A_{\parallel}$ and $A_{\perp}$ are the absorbance parallel and perpendicular to the laser polarization direction, respectively. (b) Angular dependent UV−vis spectra of PM*m*N*n* films at 320 nm; $PM_{0.9}N_{0.1}$, $PM_{0.7}N_{0.3}$, and $PM_{0.6}N_{0.4}$ films were irradiated with 35 mW cm^{-2} while $PM_{0.8}N_{0.2}$ film was irradiated with 46 mW cm^{-2}.

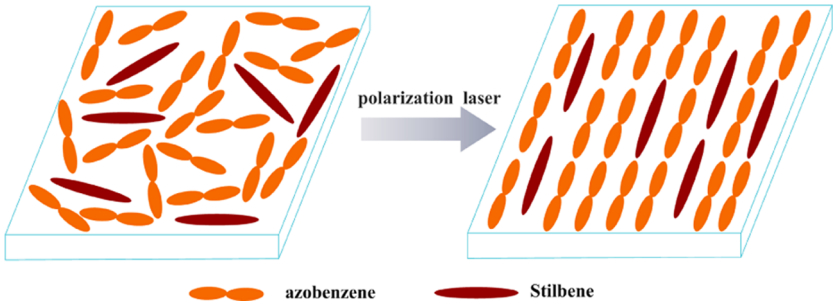

Figure 7. Schematic illustration of the photoinduced orientation process of the PM*m*N*n* films.

Anisotropic Orientation of PM*m*N*n* Films under Laser Irradiation. In this section, an s-polarized pulsed laser (355 nm) was used as the light source. As shown in Figure 6a, after irradiated with pulsed laser at 35 mW cm^{-2}, the absorbance of $PM_{0.9}N_{0.1}$ film parallel to laser polarization ($A_{\parallel}$) was smaller than that in the direction perpendicular to laser polarization ($A_{\perp}$). Figure 6b gives the angular dependent UV−vis absorption spectra of the irradiated PM*m*N*n* films at 320 nm. The absorption varied as a function of the polarization angle (polarization angle was defined as the angle between the direction of laser polarization and the direction of the polarizer). A periodical change in the absorbance with a period of 180° was seen. The maximum absorbance was present as the polarization angle was 90° and 270° while the minimum absorbance was at 180°. These results proved that the azobenzene group oriented in the direction perpendicular to the laser polarization direction. The calculated absolute value of in-plane orientation order parameter *S* were 0.200, 0.225, 0.238, and 0.285 for $PM_{0.6}N_{0.4}$, $PM_{0.7}N_{0.3}$, $PM_{0.8}N_{0.2}$, and $PM_{0.9}N_{0.1}$ films, respectively, decreasing with the content of Nstil unit increasing. It can be explained from the following two facts: first, the incorporation of Nstil group into the PM*m*N*n* film leads to the decrease of the azobenzene group, which caused the decrease of amount of oriented group. However, Nstil is no response to light due to almost no adsorption at 355 nm. Second, the order parameter *S* of azobenzene and stilbene has no significant change after annealing at 70 °C for 10 min, which indicated that the PM*m*N*n* complex does not possess the nature of the thermally induced ordered amplification effect of liquid crystalline polymer.

The orientation of Nstil unit in the complex was also detected by polarized absorption at the wavelength of 460 nm.

dx.doi.org/10.1021/ma400247h | *Macromolecules* 2013, 46, 3376−3383

Here, we take $PM_{0.6}N_{0.4}$ as an example. As shown in Figure 3, the wavelength of pulsed laser (355 nm) is far from the maximum absorption of stilbene, which avoids the absorption of stilbene. For stilbene compound without photosensitive group, orientation of stilbene group also may be obtained under light irradiation. However, it was very weak or negligible.[14,38−40] Here, the calculated absolute value of order parameter S at 460 nm was 0.151 corresponding to the stilbene group (Figure S7), much higher than that of pure stilbene film under light irradiation, indicating that the Nstil unit was driven to align via MAZO units due to the cooperative orientation. On the basis of these results, a schematic illustration of the photoresponsive processes of PM*m*N*n* complex films under irradiation with 355 nm linear pulse laser is given in Figure 7.

Fluorescence Properties of the PM*m*N*n* Films. Figure 8 and Figure S8 show the fluorescence and UV−vis spectra of the spin-coating films, respectively. The PM*m*N*n* films exhibited strong light emission under the excitation wavelength at 470 nm. The fluorescence bands were located at the wavelength of 670 nm, corresponding to a red emission. Unexpectedly, the photoluminescence intensity increased with reducing the percentage content of Nstil in the complex films. The reason for this phenomenon was that, under the irradiation of excitation light at 470 nm, the photodimerization of stilbene molecule was much easier than it fluoresces at high concentration of Nstil unit in ionic complexes.[41]

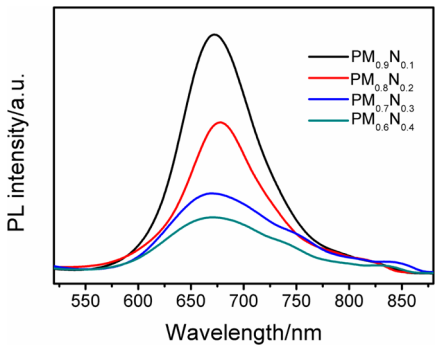

Figure 8. Fluorescence spectra of the complex films with different Nstil content. The excitation wavelength is 470 nm.

The PM*m*N*n* films with low content of Nstil still show strong fluorescence intensity though slight quenching also occurred compared with the ionic complex PM_0N_1 film without MAZO unit. For example, the fluorescence was quenched about 17% for $PM_{0.9}N_{0.1}$ with respect to PM_0N_1 film (Figure S9). Meanwhile, the fluorescent properties of PM*m*N*n* in NMP solution were also investigated, as shown in Figure S10. For the same concentration of Nstil unit, the fluorescence of PM*m*N*n* in solution was also observed with slight quenching compared to PM_0N_1 solution, i.e., 18% for $PM_{0.9}N_{0.1}$. These results are completely different with previous report on the azobenzene-containing fluorescent polymer.[42,43] That can be explained in the following aspects: the maximum absorption of azobenzene group was at 361 nm and the fluorescence emission of stilbene was 670 nm, and no overlap occurred between the fluorescence and the azobenzene unit. This feature avoids the energy transfer between the two chromophores. Moreover, the CV curves for azobenzene compound **4** shows a reduction peak at −1.62 V and stilbene compound **2** shows an oxidation peak at +0.95 V (Figure S11). The free energy ΔG for the fluorescent quenching process via the oxidative electron transfer is approximately +0.45 eV (eq S1 in Supporting Information), so that the fluorescence quenching by electron transfer may not occur.[24]

Figure 9 shows the anisotropic fluorescence emission of the PM*m*N*n* films with different Nstil content. The maximum fluorescence intensity was observed when the polarization of the excitation light was in the direction parallel to the alignment

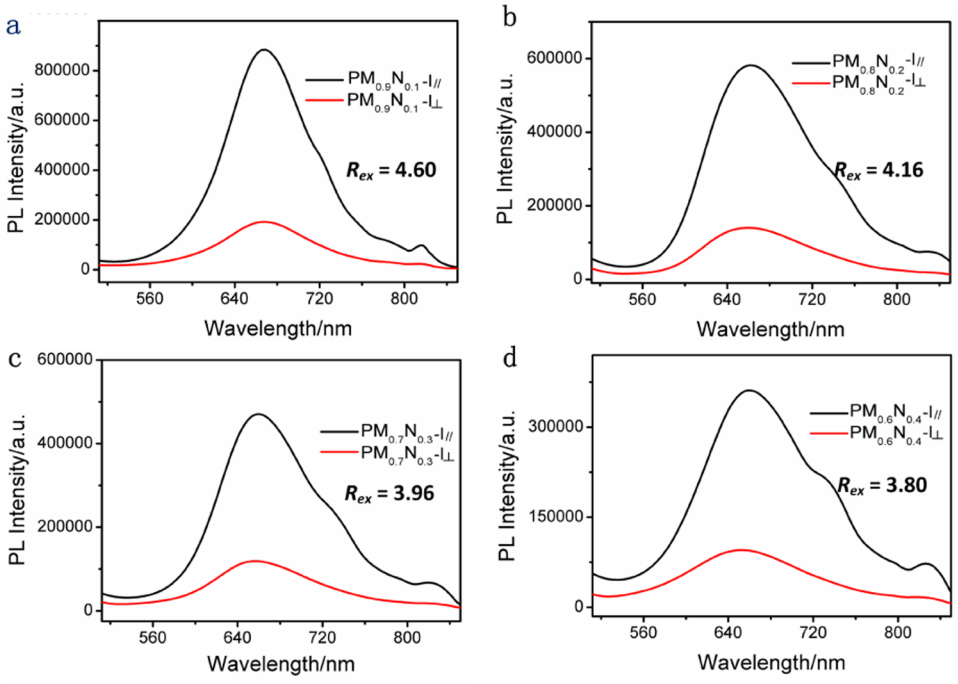

Figure 9. Polarized fluorescence spectra of the PM*m*N*n* films. $I_{\parallel}$ and $I_{\perp}$ are the fluorescence obtained by the polarization parallel and perpendicular to alignment direction of stilbene unit, respectively. All spectra were measured at room temperature, and the excitation wavelength was 470 nm.

dx.doi.org/10.1021/ma400247h | *Macromolecules* 2013, 46, 3376−3383

direction of azobenzene chromophore ($I_{\parallel}$) while the minimum fluorescence intensity in the direction perpendicular to the alignment direction of azobenzene chromophore ($I_{\perp}$). With the increase of the Nstil content in the PM*m*N*n* films, the ratio R_{ex} decreased as 4.60, 4.16, 3.96, and 3.80 for $PM_{0.9}N_{0.1}$, $PM_{0.8}N_{0.2}$, $PM_{0.7}N_{0.3}$, and $PM_{0.6}N_{0.4}$, respectively. This trend is consistent with the order parameter of azobenzene group with the change of Nstil content, further proving that the orientation of fluorescent unit Nstil was driven by the orientation of azobenzene group under linear UV light irradiation. Furthermore, the R_{ex} value did not vary with the measurements and could keep for at least 3 weeks without any change. This dichroic ratio is higher than that when a cinnamate group was employed to cooperatively orient the same fluorescent units (R_{ex} is about 2.8).[14,15] Moreover, this is significantly different from the Eu-doped azobenzene polymer film (organic–inorganic hybrid fluorescent material).[44,45] The high R_{ex} can be attributed to the high sensitivity of azobenzene group and the liquid crystalline nature of the complex. Laser treatment can cause strong thermal effect accelerating the photoinduced orientation of azobenzene groups. This result proved that laser treatment of azobenzene containing liquid crystalline materials is more effective in obtaining fluorescent film with high ratio of polarization emission.

The influence of laser fluence on the ratio R_{ex} was also investigated. The polarized fluorescence was measured on the complex films after irradiating with different laser fluence (Figure 10). The obtained curves were extremely similar to that

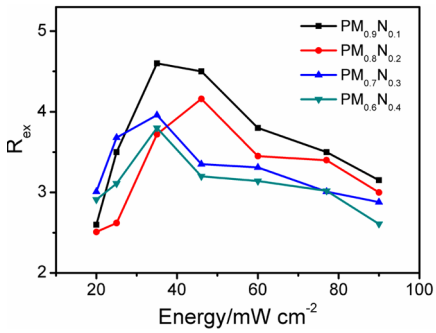

Figure 10. Influence of laser fluence on the PL dichroic ratio R_{ex} of PM*m*N*n*.

of in-plane orientation order parameter *S* as a function of the laser fluence (Figure S12). The dichroic ratio R_{ex} was first increased with the increase of the irradiation fluence and then began to decrease with the increase of laser fluence. Because the stilbene group was cooperatively oriented by azobenzene group under the irradiation of pulsed laser, the ratio R_{ex} shows trend with the order parameter *S* of MAZO unit. And the change in orientation of azobenzene with laser fluence like parabola is related to the thermal effect of the nanosecond pulsed laser. Laser irradiation leads to the anisotropic orientation of azobenzene group with a preferred direction perpendicular to the laser polarization. Meanwhile, the film surface was heated to locally melt due to the strong thermal effect of pulsed laser.[46,47] This makes the motion of azobenzene molecules and the subsequent orientation of azobenzene easy.[48] On the contrary, the thermal effect also leads to the relaxation of the oriented molecules. At low laser fluence, the thermal relaxation is rather slow and the order parameter of the orientation (*S*) increases with the laser fluence increasing. However, when irradiation dose exceeds a certain value, the thermal induced relaxation plays the major role and leads to the decrease of the orientation. The contrary factors of the pulse laser resulted in the parabola-like variation of anisotropic orientation with the laser fluence.

CONCLUSION

In this contribution, we successfully prepared fluorescence material with high polarized fluorescence emission. The material bearing azobenzene and stilbene was prepared by the ionic self-assembly approach. The fluorescence of the ionic complexes was generated without being quenched by azobenzene. The cooperative orientation of stilbene occurred following the alignment direction of azobenzene groups in the complex films irradiated by linear polarized pulsed laser. The oriented films gave the anisotropic absorption and fluorescence emission. High PL dichroic ratio R_{ex} up to 4.6 can be obtained in the complex films with the low content of Nstil unit.

ASSOCIATED CONTENT

Supporting Information

^{1}H NMR spectra of PM*m*N*n*; UV–vis spectra of the mixture M*m*N*n*; calculation for the absorption ratio A^*_{445nm}/A^*_{361nm}; The calibration curve of the A^*_{445nm}/A^*_{361nm} value vs the content of Nstil in the complexes; absorption ratio $A^*_{445nm}/A^*_{361nm}$of PM*m*N*n* and M*m*N*n*; TGA curves of MAZO, Nstil and PM*m*N*n*; POM images of PM*m*N*n*; DSC thermograms of the first and second heating curves of PM*m*N*n*; wide-angle X-ray diffraction profile of PM*m*N*n*; polarized UV–vis spectra of $PM_{0.6}N_{0.4}$; UV–vis spectra of PM*m*N*n* films; fluorescence spectra of the PM_0N_1 and $PM_{0.9}N_{0.1}$ films; fluorescence spectra of the PM*m*N*n* in NMP solution; cyclic voltammogram of compounds **4** and **2** in THF solution; influence of laser fluence on the in-plane orientation order parameter *S* of PM*m*N*n*. This material is available free of charge via the Internet at http://pubs.acs.org.

AUTHOR INFORMATION

Corresponding Author

*E-mail xueminlu@sjtu.edu.cn (X.L.), qhlu@sjtu.edu.cn (Q.L.); Fax +86 (0)21 5474 7535.

Notes

The authors declare no competing financial interest.

ACKNOWLEDGMENTS

This research project was supported by the National Science Fund for Distinguished Young Scholars (50925310), the National Science Foundation of China (51173103), 973 project (2012CB933803), and excellent academic leaders of Shanghai (11XD1403000).

REFERENCES

(1) Grell, M.; Bradley, D. D. C. *Adv. Mater.* **1999**, *11*, 895–905.
(2) Grimsdale, A. C.; Chan, K. L.; Martin, R. E.; Jokisz, P. G.; Holmes, A. B. *Chem. Rev.* **2009**, *109*, 897–1091.
(3) He, B.; Li, J.; Bo, Z.; Huang, Y. *Macromolecules* **2005**, *38*, 6762–6766.
(4) Abbas, M.; D'Amico, F.; Ali, M.; Mencarelli, I.; Setti, L.; Bontempi, E.; Gunnella, R. *J. Phys. D: Appl. Phys.* **2010**, *43*, 035103.
(5) Kwak, G.; Minakuchi, M.; Sakaguchi, T.; Masuda, T.; Fujiki, M. *Chem. Mater.* **2007**, *19*, 3654–3661.
(6) Yan, D.; Lu, J.; Wei, M.; Ma, J.; Evans, D. G.; Duan, X. *Chem. Commun.* **2009**, 6358–6360.

(7) Tian, C. H.; Zoriniants, G.; Gronheid, R.; Van der Auweraer, M.; De Schryver, F. C. *Langmuir* **2003**, *19*, 9831−9840.
(8) Simonsen, J. B.; Westerlund, F.; Breiby, D. W.; Harrit, N.; Laursen, B. W. *Langmuir* **2010**, *27*, 792−799.
(9) Pagliara, S.; Camposeo, A.; Mele, E.; Persano, L.; Cingolani, R.; Pisignano, D. *Nanotechnology* **2010**, *21*, 215304.
(10) Yin, K.; Zhang, L.; Lai, C.; Zhong, L.; Smith, S.; Fong, H.; Zhu, Z. *J. Mater. Chem.* **2011**, *21*, 444−448.
(11) Zhong, W.; Li, F.; Chen, L.; Chen, Y. W.; Wei, Y. *J. Mater. Chem.* **2012**, *22*, 5523−5530.
(12) Weder, C.; Sarwa, C.; Montali, A.; Bastiaansen, G.; Smith, P. *Science* **1998**, *279*, 835−837.
(13) Contoret, A. E. A.; Farrar, S. R.; Jackson, P. O.; Khan, S. M.; May, L.; O'Neill, M.; Nicholls, J. E.; Kelly, S. M.; Richards, G. J. *Adv. Mater.* **2000**, *12*, 971−974.
(14) Giménez, R.; Piñol, M.; Serrano, J. L.; Viñuales, A. I.; Rosenhauer, R.; Stumpe, J. *Polymer* **2006**, *47*, 5707−5714.
(15) Rosenhauer, R.; Stumpe, J.; Gimenez, R.; Pinol, M.; Serrano, J. L.; Vinuales, A.; Broer, D. *Macromolecules* **2011**, *44*, 1438−1449.
(16) Lee, J. H.; Kawatsuki, N. *Mol. Cryst. Liq. Cryst.* **2009**, *498*, 59−64.
(17) Lee, J.; Matsuda, S.; Kawatsuki, N. *Mol. Cryst. Liq. Cryst.* **2010**, *529*, 20−24.
(18) Neill, M. O.; Kelly, S. M. *J. Phys. D: Appl. Phys.* **2000**, *33*, R67−84.
(19) Natansohn, A.; Rochon, P. *Chem. Rev.* **2002**, *102*, 4139−4175.
(20) Ikeda, T.; Mamiya, J.; Yu, Y. *Angew. Chem., Int. Ed.* **2007**, *46*, 506−528.
(21) Li, C.; Zhang, Y.; Ju, J.; Cheng, F.; Liu, M.; Jiang, L.; Yu, Y. *Adv. Funct. Mater.* **2012**, *22*, 760−763.
(22) Bandara, H. M. D.; Burdette, S. C. *Chem. Soc. Rev.* **2012**, *41*, 1809−1825.
(23) Vögtle, F.; Gorka, M.; Hesse, R.; Ceroni, P.; Maestri, M.; Balzani, V. *Photochem. Photobiol.* **2002**, *1*, 45−51.
(24) Ceroni, P.; Laghi, I.; Maestri, M.; Balzani, V.; Gestermann, S.; Gorkab, M.; Vögtle, F. *New J. Chem.* **2002**, *26*, 66−75.
(25) Gimenez, R.; Millaruelo, M.; Pinol, M.; Serrano, J. L.; Vinuales, A.; Rosenhauer, R.; Fischer, T.; Stumpe, J. *Polymer* **2005**, *46*, 9230−9242.
(26) Harbron, E. J.; Vicente, D. A.; Hoyt, M. T. *J. Phys. Chem. B* **2004**, *108*, 18789−18792.
(27) Abdallah, D.; Whelan, J.; Dust, J. M.; Hoz, S.; Buncel, E. *J. Phys. Chem. A* **2009**, *113*, 6640−6647.
(28) Schuster, D. I.; Li, K.; Guldi, D. M.; Palkar, A.; Echegoyen, L.; Stanisky, C.; Cross, R. J.; Niemi, M.; Tkachenko, N. V.; Lemmetyinen, H. *J. Am. Chem. Soc.* **2007**, *129*, 15973−15982.
(29) Hara, Y.; Fujii, T.; Kashida, H.; Sekiguchi, K.; Liang, X.; Niwa, K.; Takase, T.; Yoshida, Y.; Asanuma, H. *Angew. Chem., Int. Ed.* **2010**, *49*, 5502−5506.
(30) Astruc, D.; Boisselier, E.; Ornelas, C. *Chem. Rev.* **2010**, *110*, 1857−1959.
(31) Archut, A.; Azzellini, G. C.; Balzani, V.; De Cola, L.; Vögtle, F. *J. Am. Chem. Soc.* **1998**, *120*, 12187−12191.
(32) Dube, H.; Ams, M. R.; Rebek, J. *J. Am. Chem. Soc.* **2010**, *132*, 9984−9985.
(33) Jager, W. F.; Sarker, A. M.; Neckers, D. C. *Macromolecules* **1999**, *32*, 8791−8799.
(34) Xiao, S. F.; Lu, X. M.; Lu, Q. H.; Su, B. *Macromolecules* **2008**, *41*, 3884−3892.
(35) Yoshino, N.; Kitamura, M.; Seto, T.; Shibata, Y.; Abe, M.; Ogino, K. *Bull. Chem. Soc. Jpn.* **1992**, *65*, 2141−2144.
(36) Zhang, Q.; Bazuin, C. G.; Barrett, C. J. *Chem. Mater.* **2008**, *20*, 29−31.
(37) Zhang, Q.; Bazuin, C. G. *Macromolecules* **2009**, *42*, 4775−4786.
(38) Fischer, T.; Ruhmann, R.; Seeboth, A. *J. Chem. Soc., Perkin Trans. 2* **1996**, 1087−1090.
(39) Wolarz, E.; Fischer, T.; Stumpe, J. *Thin Solid Films* **2003**, *424*, 179−185.
(40) Ilieva, D.; Nedelchev, L.; Petrova, T.; Dragostinova, V.; Todorov, T.; Nikolova, L.; Ramanujam, P. S. *J. Opt. A: Pure Appl. Opt.* **2006**, *8*, 221−224.
(41) Aguiar, M.; Hu, B.; Karasz, F. E.; Akcelrud, L. *Macromolecules* **1996**, *29*, 3161−3166.
(42) Rosenhauer, R.; Fischer, T.; Stumpe, J.; Gimenez, R.; Pinol, M.; Serrano, J. L.; Vinuales, A.; Broer, D. *Macromolecules* **2005**, *38*, 2213−2222.
(43) Liu, X. G.; Feng, Y. Q.; Zhao, Y.; Chen, H. L.; Li, X.-G. *Dyes Pigm.* **2007**, *75*, 413−419.
(44) Wu, S.; Yu, X.; Huang, J.; Shen, J.; Yan, Q.; Wang, X.; Wu, W.; Luo, Y.; Wang, K.; Zhang, Q. *J. Mater. Chem.* **2008**, *18*, 3223−3229.
(45) Yan, Q.; Wu, Y.; Wang, X.; Luo, Y.; Zou, G.; Zhang, Q. *J. Polym. Res.* **2010**, *17*, 707−712.
(46) Evans, K. E. *J. Appl. Phys.* **1988**, *63*, 4946−4950.
(47) Bartholomeusz, B. J. *Appl. Opt.* **1992**, *31*, 909−918.
(48) Li, X.; Lu, X. M.; Lu, Q. H.; Yan, D. Y. *Macromolecules* **2007**, *40*, 3306−3312.